Available online at www.sciencedirect.com
ScienceDirect
European Journal of Mechanics B/Fluids 26 (2007) 330–343

Optimal disturbances in suction boundary layers

Martin G. Byström, Ori Levin, Dan S. Henningson *

Department of Mechanics, Royal Institute of Technology (KTH), SE-100 44, Stockholm, Sweden

Received 9 June 2005; accepted 9 July 2006

Available online 20 October 2006

Abstract

A well-known optimization procedure is used to find the optimal disturbances in two different suction boundary layers within the spatial framework. The maximum algebraic growth in the asymptotic suction boundary layer is presented and compared to previous temporal results. Furthermore, the spatial approach allows a study of a developing boundary layer in which a region at the leading edge is left free from suction. This new flow, which emulates the base flow of a recent wind-tunnel experiment, is herein denoted a semi-suction boundary layer. It is found that the optimal disturbances for these two suction boundary layers consist of streamwise vortices that develop into streamwise streaks, as previously found for a number of shear flows. It is shown that the maximum energy growth in the semi-suction boundary layer is obtained over the upstream region where no suction is applied. The result indicates that the spanwise scale of the streaks is set in this region, which is in agreement with previous experimental findings.

PACS: 47.15.Cb; 47.15.Fe; 47.20.Ft

Keywords: Suction boundary layer; Optimal disturbance; Algebraic growth; Streamwise streaks; Free-stream turbulence

1. Introduction

The transition from laminar to turbulent flow is a critical process in any engineering application where the minimization of friction drag is a design objective. Transition prediction has traditionally been carried out by considering the unstable eigenmodes of the Orr–Sommerfeld equations, i.e. the exponentially growing Tollmien–Schlichting waves. However, under certain circumstances other transition scenarios are more likely. It is well known that elongated, streamwise-oriented structures of alternating low and high velocity develop in boundary layers subjected to high or moderate levels of free-stream turbulence. These structures are commonly referred to as streaks or Klebanoff modes after the experiments of Klebanoff [1]. Since then, a number of experimental studies have shown that these streaks grow algebraically in the downstream direction [2–4]. Due to secondary instabilities, they break down to turbulence when their amplitude reach a critical level [5–7]. The physical mechanism behind the formation of streaks was first explained by Landahl [8,9]. He argued that when a fluid element is lifted up in the wall-normal direction it will initially maintain its horizontal momentum. Hence, small perturbations in the wall-normal direction can cause large

* Corresponding author.
E-mail address: henning@mech.kth.se (D.S. Henningson).

0997-7546/$ – see front matter
doi:10.1016/j.euromechflu.2006.07.003

disturbances in the streamwise direction. This mechanism is commonly referred to as the *lift-up* effect. Ellingsen and Palm [10] showed theoretically that three-dimensional disturbances can grow linearly with time in an inviscid flow without inflection point.

Among the first to calculate optimal perturbations numerically were Butler and Farrel [11] and Reddy and Henningson [12]. Butler and Farrel [11] considered the temporal development of linear, three-dimensional perturbations in a number of shear flows. They used a variational method to find the optimal perturbations, i.e. the perturbations that gain the most energy in a given time period. It was found that these perturbations resemble streamwise vortices that give rise to streamwise streaks. Corbett and Bottaro [13,14] calculated the optimal perturbation of the Falkner–Skan boundary layer and later the Falkner–Skan–Cooke boundary layer within the temporal framework. The spatial framework is however more physically relevant than the temporal, it has also the advantage of allowing studies of non-parallel flows such as the developing Blasius boundary layer (BBL). Andersson et al. [15] and Luchini [16] separately calculated the optimal disturbance in the non-parallel BBL. The disturbance was introduced at the leading edge and it was found that the optimal disturbance consists of streamwise aligned vortex pairs developing into streaks. Levin and Henningson [17] extended the work of Andersson et al. [15] to the Falkner–Skan boundary layer. The disturbance was however not initiated at the leading edge, but at a downstream position optimized to give the highest possible growth.

One method to delay transition is to apply suction through the surface which the boundary layer develops over. The suction can be optimized to minimize the growth of different types of disturbances [18–20]. Herein we will however study the algebraic disturbance growth in boundary layers where uniform suction is applied. When uniform suction is applied over a flat plate, the boundary layer will asymptotically approach the asymptotic suction boundary layer (ASBL), as outlined in Schlichting [21]. Fransson and Alfredsson [22] made an experimental study on the algebraic growth of disturbances induced by free-stream turbulence in the ASBL. A small region at the leading edge was however free from suction, allowing a BBL to develop up to the point where the suction set in. Downstream of this point the flow evolved into the ASBL, which was reached within the upstream half of the measurement interval. In the present paper, we will denote this type of boundary layer, where suction is applied only over the downstream part of the interval, a semi suction boundary layer (SSBL). Fransson and Alfredsson [22] compared the disturbance growth in the BBL and the SSBL. The disturbance energy was found to grow linearly in the downstream direction, but when suction was applied the growth ceased so that the present amplitude level was kept essentially constant. The suction also resulted in a twofold reduction of the boundary-layer thickness, despite of this the spanwise scale of the streaks was maintained. Fransson and Alfredsson [22] argue that the initial spanwise scale is decided in the receptivity process, this would explain the similarity of scales since a BBL is present at the leading edge of the SSBL. Yoshioka et al. [23] extended the work of Fransson and Alfredsson [22] to a number of turbulence levels, free-stream and suction velocities. They found that the wall suction suppresses the disturbance growth, for high suction rates the disturbance energy may even decay. For conditions similar to those of the experiment by Fransson and Alfredsson [22], it was concluded that the disturbances initiated at the leading edge become mainly passive and are convected downstream by the flow without changing the spanwise scale. However, Yoshioka et al. [23] argue that the spanwise scale of the streaks approach the optimal scale in the ASBL when the conditions are such that the difference in displacement thickness between the upstream and downstream region is small. Fransson and Corbett [24] used an adjoint-based optimization procedure [14] to calculate the optimal perturbation in the ASBL within the temporal framework. The optimal velocity perturbation was found to be in good agreement with experimental data from Fransson and Alfredsson [22], but there was some discrepancy between the optimal wavenumber and those experimentally observed.

In the present paper we calculate the optimal disturbances in the ASBL and the SSBL within the spatial context. The calculations are carried out with an adjoint-based optimization procedure implemented by Levin and Henningson [17], valid in the large Reynolds-number limit for a viscous, incompressible flow. Furthermore, the spanwise wavenumber and angular frequency of the disturbance as well as the streamwise interval length are optimized. The current study was motivated by the wind-tunnel experiment by Fransson and Alfredsson [22]. Results from this experiment have previously been compared with the temporal study of the ASBL by Fransson and Corbett [24]. This study was however restricted to a non-developing base flow. The spatial approach used herein allows us to simulate the actual base flow of the experiments, i.e. the SSBL. A comparison of the optimal disturbances in the ASBL and the SSBL is then carried out to establish the effect of the differences between these two suction boundary layers.

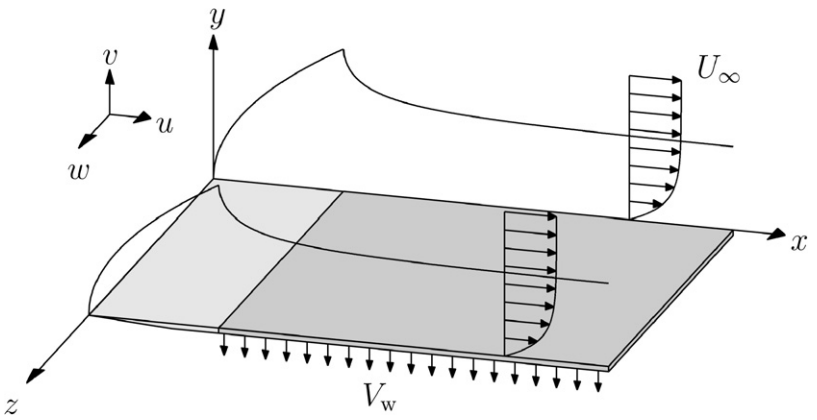

Fig. 1. The semi suction boundary layer (SSBL).

2. General formulation

We study the growth of optimal disturbances in a flat plate boundary layer where suction is applied at the wall. As seen in Fig. 1, we denote the streamwise, wall-normal and spanwise coordinates x, y and z and the corresponding velocities u, v and w, respectively. The time is denoted t, the pressure p, the spanwise wavenumber and the angular frequency are denoted β and ω. The kinematic viscosity and the density of the fluid are denoted ν and ρ.

The base flow of the ASBL is given by a simple analytic expression, first derived by Griffith and Meredith [25]

$$U = U_\infty\left(1 - \exp\left[\frac{V_w}{\nu}y\right]\right), \qquad V = V_w, \tag{1}$$

where U_∞ is the free-stream velocity and V_w is the suction velocity at the wall, which assumes a negative value when suction is applied. This velocity profile is an exact solution to both the full Navier–Stokes equations and the boundary-layer equations. The displacement thickness δ_1 of the ASBL is constant since the base flow does not vary in the streamwise direction. The Reynolds number based on this constant displacement thickness can also be written as the ratio between the free-stream velocity and the suction velocity, from here on we will refer to this as the suction Reynolds number Re

$$\delta_1 = -\frac{\nu}{V_w}, \qquad Re = \frac{U_\infty\delta_1}{\nu} = -\frac{U_\infty}{V_w}. \tag{2}$$

Herein we will use a scaling based on the constant displacement thickness of the ASBL to scale both mean flow and disturbances. This scaling, summarized in Table 1, will be referred to as the ASBL scalings. From here on we will use the superscript * to distinguish non-scaled, physical quantities from those scaled in accordance with Table 1. Using scaled quantities we may rewrite Eq. (1)

$$U = \frac{U^*}{U_\infty} = 1 - \exp\left[-\frac{y^*}{\delta_1}\right] = 1 - \exp[-y], \qquad V = \frac{V_w^*}{U_\infty}Re = V_w. \tag{3}$$

The base flow of the SSBL can be divided into two regions. In the first region, from the leading edge to the position where the suction starts, the base flow was obtained by solving the Blasius similarity equation. In the second region, where suction is applied, the base flow was obtained by numerically solving the boundary-layer equations. The streamwise velocity is subjected to homogeneous boundary conditions at the wall, the boundary condition for the wall-normal component is given by the suction velocity V_w. We scale the SSBL with the ASBL scalings given by Table 1. The Reynolds number $Re = -U_\infty/V_w$ is however not physically relevant in the upstream region where no suction is applied. The BBL of this region has previously been studied by Andersson et al. [15], Luchini [16] and Levin and Henningson [17]. They used boundary-layer scalings and defined a Reynolds number $Re_l = U_\infty l/\nu$, where l is a fixed streamwise distance that is also used to scale x. In the SSBL, the natural choice for l is the distance between

Table 1
The ASBL scalings

Variable	x	y, z	t	u	v, w	p	β	ω
Scaling	$\delta_1 Re$	δ_1	$\delta_1 Re/U_\infty$	U_∞	U_∞/Re	$\rho U_\infty^2/Re^2$	$1/\delta_1$	$U_\infty/(\delta_1 Re)$

the leading edge and the point where the suction starts. Writing the starting position of the suction, x_s, with the ASBL scalings from Table 1

$$x_s = \frac{x_s^*}{\delta_1 Re} = \frac{l}{\delta_1 Re} = \frac{Re_l}{Re^2}, \tag{4}$$

we find that changing the starting position of the suction is equivalent to changing Re_l, given that Re is kept constant. In the study of the SSBL presented in Section 3.1 we set x_s to unity in order to comply with the experiments by Fransson and Alfredsson [22]. Setting x_s to unity is equivalent to setting $Re_l = Re^2$, this is beneficiary since it means that quantities scaled with the ASBL scalings can be directly compared to quantities scaled with the boundary-layer scalings and vice versa. Further details on the base flow of the SSBL will be given in Section 3.1.1.

For these two-dimensional steady base flows, the SSBL and the ASBL, we consider three-dimensional and time-dependent disturbances. The disturbances are taken to be periodic in the spanwise direction and in time. We consider algebraically growing disturbances with weak streamwise variation, the streamwise wavenumber is thus set to zero. Either one of the disturbances u, v, w or p can then be assumed to be of the form

$$f = \hat{f}(x, y) \exp[\mathrm{i}\beta z - \mathrm{i}\omega t]. \tag{5}$$

Introducing this assumption in the non-dimensional, linearized Navier–Stokes equations and neglecting terms of low order yields a parabolic set of disturbance equations as outlined in Levin and Henningson [17]. The disturbance is subjected to no-slip boundary conditions at the wall, the wall-normal disturbance can be set to zero since we consider suction through a material of low permeability [24]. Together with boundary and initial conditions, the disturbance equations form an initial boundary-value problem that can be solved through downstream marching for a disturbance with given spanwise wavenumber and angular frequency.

The aim is to optimize the initial disturbance $(\hat{u}_0, \hat{v}_0, \hat{w}_0)$ at x_0, the beginning of the interval, in order to achieve maximum possible amplification of the disturbance energy at x_1, the end of the interval. We define the growth G over the interval $x_0 \leqslant x \leqslant x_1$ as the ratio between the disturbance energy E at the end and beginning of the interval.

$$G(x_0, x_s, x_1, \beta, \omega, Re) = \frac{E(x_1)}{E(x_0)}. \tag{6}$$

Observe that the growth in the ASBL will not depend on the position where the suction starts, x_s, since we assume that it is located sufficiently far upstream so that the ASBL has been reached at the start of the interval. The energy norm E is defined in the same way as stated in Andersson et al. [15], Luchini [16] and Levin and Henningson [17]. As outlined in these papers, in a high Reynolds-number flow the highest possible growth is achieved for an initial disturbance with a zero streamwise component, due to the difference in order between the streamwise component and the wall-normal and spanwise components. This difference in order also makes it possible to neglect the wall-normal and spanwise components at the end of the interval. It then follows that the growth scales quadratically with Re in the large Reynolds-number limit [15–17].

Since the initial boundary-value problem is linear and homogeneous an input–output formulation can be adopted, such that the disturbance at the final position is a linear function of the initial disturbance. By introducing the adjoint equations, the optimal initial disturbance and the associated growth can be calculated through power iterations. The optimization procedure used herein to calculate the optimal disturbances in the SSBL and the ASBL was implemented by Levin and Henningson [17]. It is similar to the procedures that were used by Andersson et al. [15] and Luchini [16]. A detailed description of this procedure can also be found in the textbook by Schmid and Henningson [26].

3. Results

All results presented in this section have been subjected to convergence tests in order to ensure their accuracy. Furthermore, the height of the calculation box y_{max} was varied between 40 and 60 to make sure that the whole initial disturbance was captured.

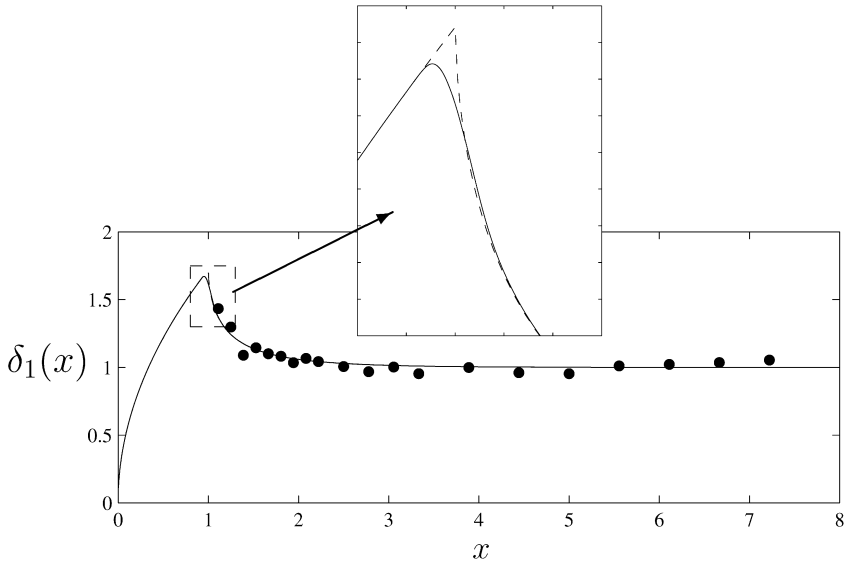

Fig. 2. The displacement thickness $\delta_1(x)$ of the SSBL at $Re = 347$, scaled with the constant displacement thickness of the ASBL. Discontinuous flow (dashed line) and approximated continuous flow with smoothly applied suction (solid line). Experimental data from Fransson and Alfredsson [22] (dots).

3.1. The semi suction boundary layer

3.1.1. Base flow

In this section we study the SSBL in which a BBL develops from the leading edge to the point where the suction starts. Downstream of this point a uniform suction is applied, in this evolution region the flow evolves towards the ASBL. The streamwise distance needed for the flow to reach the ASBL is decided by the strength of the suction and the thickness of the BBL at the position where the suction starts. The SSBL emulates the base flow of an experiment carried out by Fransson and Alfredsson [22]. In this experiment, the boundary layer developed over a flat plate made of porous material so that suction could be applied. The leading edge was however made of an impermeable material, leaving this region free from suction. Fransson and Alfredsson [22] set the suction Reynolds number to $Re = 347$ and started the suction 360 mm downstream of the leading edge, equivalent to setting $x_s = x_s^*/(\delta_1 Re)$ to unity. As outlined in Section 2, this allows us to make direct comparisons with quantities scaled with the boundary-layer scalings. Herein we study the SSBL over nine streamwise intervals, all starting at $x_0 = 0$ and with suction from $x_s = 1$ to the end of the interval. The length of the interval is varied by changing the end position from $x_1 = 2$ to $x_1 = 10$ in steps of one.

Fransson and Alfredsson [22] used a non-dimensional evolution equation to calculate the base flow of the evolution region between the BBL and the ASBL. The exact agreement with their results validated the numerical solver of the boundary-layer equations that was used in the present implementation. A small modification of the base flow was however made since the SSBL is discontinuous at $x_s = 1$ where the suction starts. In order to remove this discontinuity, we employ a strategy previously used by Zuccher et al. [20] and Corbett and Bottaro [27], using a step function to smoothly increase the suction from zero at $x = 0.9$ to full suction at $x = 1.1$. The used step function [28] has continuous derivatives of all orders and gives the same mass flux through the wall as the discontinuous flow. Fig. 2 shows a comparison of the displacement thickness of the discontinuous flow and the modified continuous flow with smoothly applied suction. Despite the smooth application of the suction, the flow undergoes a significant transformation over a short streamwise distance, a finer grid was therefore used in this region and at the leading edge. Experimental data from Fransson and Alfredsson [22] is also included in Fig. 2, good agreement can be seen between the calculated and measured displacement thickness.

Another approximation was done in the treatment of the leading edge. The limit of the normal velocity of the BBL is infinity when x tends towards zero. However, here we follow the work of Andersson et al. [15] and set the normal velocity to zero and the streamwise velocity to unity at the initial point of the calculation interval.

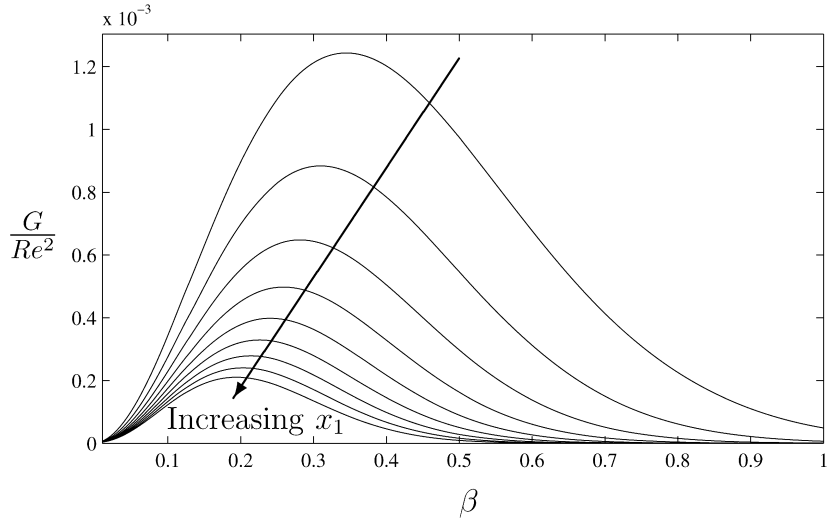

Fig. 3. The growth G in the SSBL at $Re = 347$ as function of β for nine streamwise intervals ranging from $0 \leqslant x \leqslant 2$ to $0 \leqslant x \leqslant 10$ in steps of one.

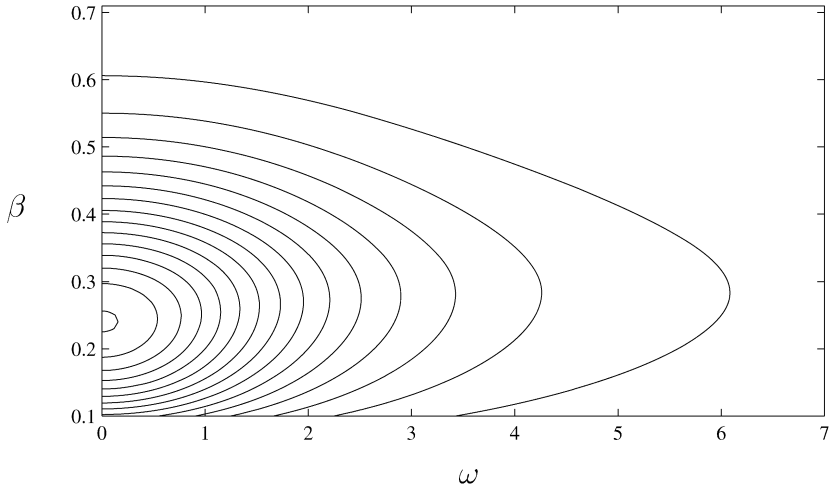

Fig. 4. Contours of constant growth G in the SSBL at $Re = 347$ in the (ω, β)-plane for the streamwise interval $0 \leqslant x \leqslant 6$.

3.1.2. Optimal disturbances

The influence of the spanwise wavenumber β and the angular frequency ω on the energy growth in the SSBL was studied for the nine streamwise intervals defined in Section 3.1.1. Apart from when the ω-dependence is studied, ω is set to zero for all calculations presented in this section.

Fig. 3 shows the growth as function of β for all nine streamwise intervals. We gather that the optimal growth occurs at different β for each respective interval, i.e. for each streamwise interval there is an optimal β that gives the largest possible growth at the end of that interval. This optimal β and the corresponding optimal growth decrease as the interval is prolonged. The optimal spanwise wavenumbers and the corresponding optimal growth are summarized in Table 2, Section 3.2.

The ω-dependence is exposed in Fig. 4, which shows contours of constant growth in the (ω, β)-plane for the streamwise interval $0 \leqslant x \leqslant 6$. From the figure we conclude that the optimal ω is zero, this conclusion was found to be true for all the streamwise intervals studied here. This is in agreement with what has been found for the BBL by Luchini [16] and the Falkner–Skan boundary layer by Levin and Henningson [17].

The growth as function of the streamwise coordinate x is shown in Fig. 5 for all nine streamwise intervals. The optimal β of each respective interval was used in these calculations and ω was set to zero. The optimization procedure

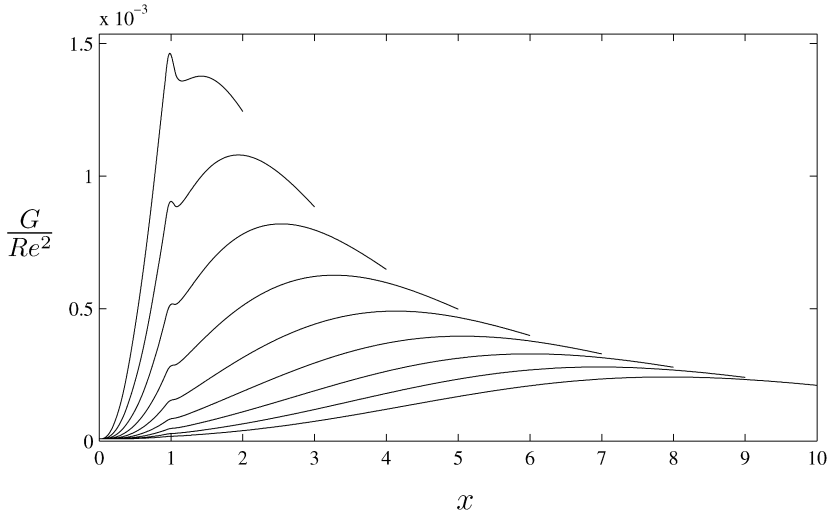

Fig. 5. The growth G in the SSBL at $Re = 347$ as function of x for nine streamwise intervals ranging from $0 \leqslant x \leqslant 2$ to $0 \leqslant x \leqslant 10$ in steps of one. The optimal β of each respective interval was used, ω was set to zero.

used herein optimizes the growth at the end of the streamwise interval. The optimal growth is thus the largest possible growth at the end of the streamwise interval but does not necessarily constitute the largest growth in the interval. As seen in Fig. 5 each curve has a maximum upstream of their respective end position and these maxima exceed the optimal growth for all intervals. The maxima are located in the suction part of the SSBL, except for the shortest interval ($0 \leqslant x \leqslant 2$), which has the maximum located at the starting point of the suction, i.e. at the end of the BBL. When the endpoint of the interval was moved further upstream, towards the starting point of the suction, it was found that the maximum remains located at this point. Due to the smooth application of the suction (see Section 3.1.1), the maximum growth is reached slightly upstream of $x_s = 1$. It is however reasonable to assume that the maximum growth will be reached at exactly $x_s = 1$ in the discontinuous flow. The optimal interval for the SSBL thus ends at the point where the suction starts. In this interval, where no suction is applied, the base flow is simply the BBL for which it is well known that the optimal spanwise wavenumber is $\beta = 0.45$ (Andersson et al. [15], Luchini [16]).

Fig. 6 shows the optimal disturbances in the SSBL for the streamwise intervals $0 \leqslant x \leqslant 2$ (solid line), $0 \leqslant x \leqslant 6$ (dashed line) and $0 \leqslant x \leqslant 10$ (dotted line). For each respective interval the optimal β was used and ω was set to zero. Figs. 6(a), (b) show the optimal disturbance while Fig. 6(c) shows the downstream response of the optimal disturbance at the final position. The downstream response takes the form of a streamwise elongated streak when the spanwise periodic dependence is considered. The amplitude of the streak is larger for short intervals than for long, but the shape of the streak remains similar and the profile maximum is located at about the same wall-normal distance from the wall, where the SSBL reaches approximately three quarters of the free-stream velocity. From this we conclude that there is an optimal shape, a streak located at a certain wall-normal position, that gives the highest disturbance energy at the end of the interval.

The optimal disturbance, i.e. the wall-normal and spanwise components shown in Figs. 6(a), (b), takes the form of streamwise aligned vortex pairs when the spanwise periodic dependence is considered. We also observe that the profile maxima move upward when the streamwise interval is prolonged. Thus, the vortex cores of the initial disturbance move upward and the vortices grow in size, as seen in Fig. 7. An explanation for this is that the suction will draw the disturbance towards the wall as it evolves downstream. From Fig. 6(c) we saw that the downstream response of the optimal disturbance is a streak located at a certain optimal wall-normal position. The cores of the vortices, i.e. the optimal disturbance, must be located some distance higher in the wall-normal direction in order to allow the suction to draw the disturbance down to this optimal wall-normal position as it evolves over the interval. This effect is stronger for longer streamwise intervals where the suction will act on the disturbance over a longer distance. The vortex cores must therefore be located higher for a long interval than for a short in order for the disturbance to reach the optimal wall-normal coordinate at the end of the interval.

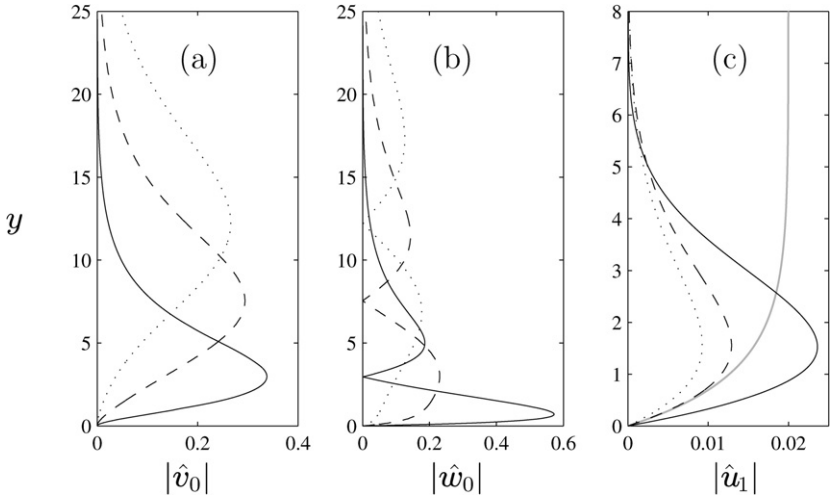

Fig. 6. The optimal disturbance in the SSBL at $Re = 347$ and for the streamwise intervals $0 \leqslant x \leqslant 2$ (solid line), $0 \leqslant x \leqslant 6$ (dashed line) and $0 \leqslant x \leqslant 10$ (dotted line). (a–b) The wall-normal component $\hat{v}_0$ and the spanwise component $\hat{w}_0$ of the optimal disturbance. (c) The downstream response of the optimal disturbance, streamwise component $\hat{u}_1$. Observe that the scaling of $\hat{u}$ differs a factor Re from the scaling of $\hat{v}$ and $\hat{w}$, see Section 2. The grey line shows the ASBL, scaled down to fit the figure. The ASBL has been reached (within graphical accuracy) at the end of the streamwise intervals examined here.

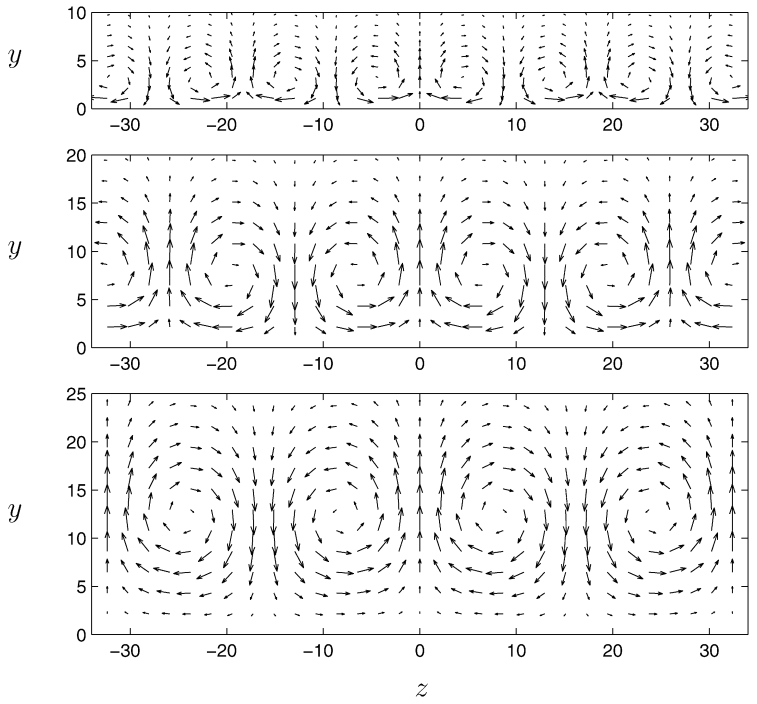

Fig. 7. The optimal disturbance in the SSBL at $Re = 347$ for the streamwise intervals $0 \leqslant x \leqslant 2$ (upper row), $0 \leqslant x \leqslant 6$ (middle row) and $0 \leqslant x \leqslant 10$ (bottom row).

3.2. A comparison with the asymptotic suction boundary layer

In this section we study the energy growth of the optimal disturbance in the ASBL and make a comparison between the SSBL and the ASBL. We study the ASBL over the same streamwise intervals that were used for the SSBL, although the suction is here applied over the whole interval. Since the base flow of the ASBL does not vary in the

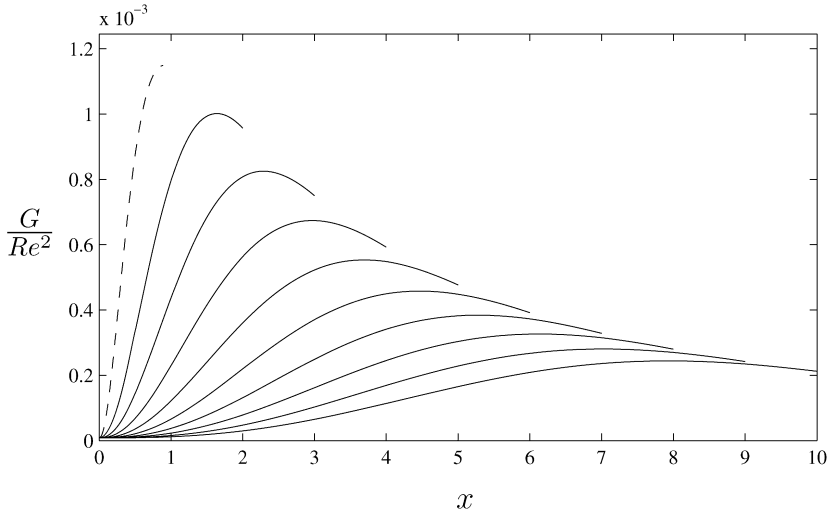

Fig. 8. The growth G in the ASBL as function of x at $Re = 347$ for nine streamwise intervals ranging from $0 \leqslant x \leqslant 2$ to $0 \leqslant x \leqslant 10$ in steps of one (solid lines) and for the optimal interval $0 \leqslant x \leqslant 0.89$ (dashed line). The optimal β of each respective interval was used in these calculations and ω was set to zero.

streamwise direction (see Section 2), it is however arbitrary which interval we study as long as we keep the length constant. The Reynolds number Re was set to 347, as in the study of the SSBL.

The optimal disturbance in the ASBL takes the form of streamwise aligned vortex pairs that give rise to streamwise elongated streaks. This is in agreement with the results from the temporal study of the ASBL by Fransson and Corbett [24]. The dependence on the spanwise wavenumber β resembles that found for the SSBL (see Table 2) and the optimal angular frequency ω was found to be zero irrespective of the interval length. Fig. 8 shows the growth as function of the streamwise coordinate for all nine streamwise intervals, the optimal β for each respective interval was used in these calculations and ω was set to zero. For all the intervals the optimal growth is exceeded by maxima upstream of the endpoints. An optimization of the endpoint of the streamwise interval was therefore carried out, it was found that the largest possible growth of $G = 0.11 \times 10^{-2} Re^2$ occurs when $x_1 = 0.89$ and $\beta = 0.52$, the dashed line in Fig. 8. This result can be compared with the temporal study of the ASBL by Fransson and Corbett [24]. They found that the optimal disturbance, with $\beta = 0.53$, gives rise to a growth of $G = 0.99 \times 10^{-3} Re^2$ over the optimal temporal interval. The spatial growth presented here is 16% higher than this temporal result. Biau and Bottaro [29], who carried out a study on optimal disturbances in the plane Poiseuille flow, also found that spatial analysis gives higher growth than the temporal analysis. The plane Poiseuille flow was implemented herein and the growth calculated for the optimal wavenumber and interval given by Biau and Bottaro [29]. The result matched that of Biau and Bottaro [29] and thus validated the used optimization procedure.

It is interesting to compare the optimal disturbance in the SSBL with that in the ASBL since it will expose how the differences in the base flow at the beginning of the interval affect the disturbance as it evolves downstream. One would expect that the differences between the disturbances will go towards zero as the streamwise interval is prolonged since the base flow of the SSBL approaches that of the ASBL.

The left column of Fig. 9 shows the growth as function of the spanwise wavenumber β for both the SSBL (solid line) and the ASBL (dashed line) while the right column shows the growth as function of the streamwise coordinate x. The angular frequency ω was set to zero and the optimal β was used when the growth as function of x was calculated. Three different streamwise intervals were used, $0 \leqslant x \leqslant 2$, $0 \leqslant x \leqslant 6$ and $0 \leqslant x \leqslant 10$. For the shortest interval, shown in the upper row, the SSBL gives a 30% higher optimal growth than the ASBL. The optimal growth also occurs at a lower spanwise wavenumber for the SSBL than for the ASBL. Studying the growth as function of x, we gather that the reason for the large difference in growth is the contribution from the BBL at the beginning of the SSBL. The middle row shows the interval $0 \leqslant x \leqslant 6$, for this interval the curves lie much closer, but the SSBL still gives a slightly higher optimal growth than the ASBL. The optimal spanwise wavenumber is however the same. The contribution from the BBL is also much smaller, this explains why the optimal growth in the SSBL ends up so much closer to that in the ASBL. Finally we examine the long streamwise interval $0 \leqslant x \leqslant 10$, shown in the bottom row of Fig. 9. The

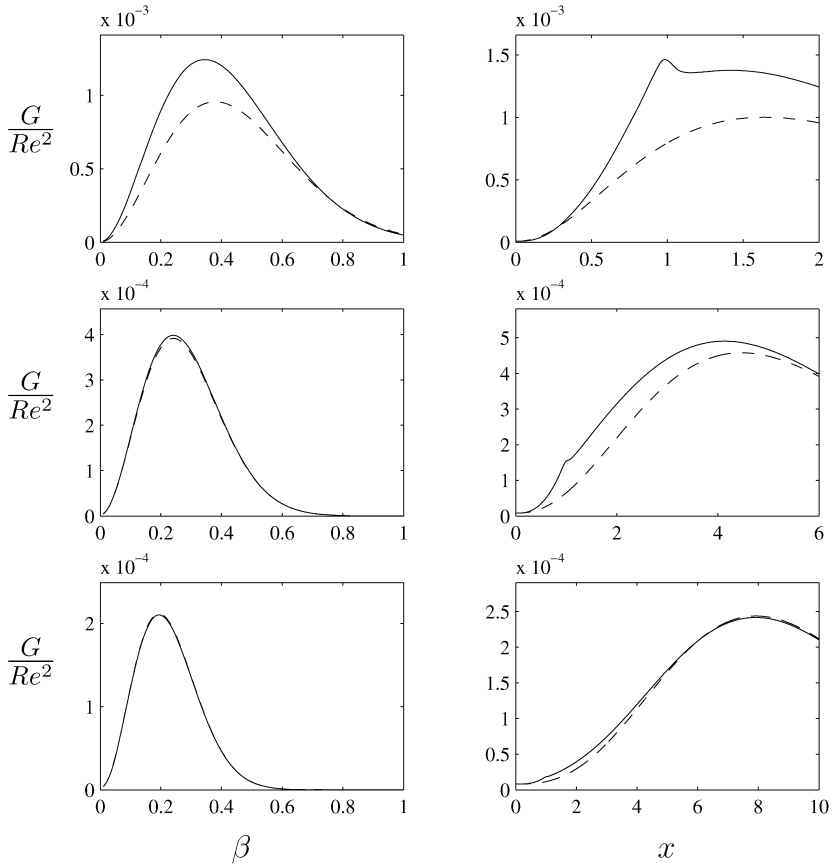

Fig. 9. Left column: the growth G as function of β. Right column: the growth of the disturbance with optimal β as function of x. The SSBL (solid line) and the ASBL (dashed line) at $Re = 347$. The upper, middle and bottom row shows the growth in the streamwise intervals $0 \leqslant x \leqslant 2$, $0 \leqslant x \leqslant 6$ and $0 \leqslant x \leqslant 10$, respectively.

Table 2
The optimal growth and spanwise wavenumber in the ASBL and the SSBL at $Re = 347$ for nine streamwise intervals of different length

x_1	2	3	4	5	6	7	8	9	10
β_{ASBL}	0.38	0.32	0.29	0.26	0.24	0.23	0.21	0.20	0.19
β_{SSBL}	0.35	0.31	0.28	0.26	0.24	0.23	0.21	0.20	0.19
$G_{\mathrm{ASBL}}/Re^2 \times 10^2$	0.096	0.075	0.059	0.048	0.039	0.033	0.028	0.024	0.021
$G_{\mathrm{SSBL}}/Re^2 \times 10^2$	0.12	0.088	0.065	0.050	0.040	0.033	0.028	0.024	0.021

curves collapse when we study the growth as function of the spanwise wavenumber, but a small difference can still be seen at the beginning of the streamwise interval. A more detailed comparison is done in Table 2, which states the optimal spanwise wavenumber and corresponding optimal growth for all streamwise intervals. We conclude that the optimal growth and spanwise wavenumber in the SSBL go towards those in the ASBL when the streamwise interval is prolonged.

In Fig. 10 we compare the optimal disturbance in the SSBL (solid lines) and the ASBL (dashed lines). The upper row shows the wall-normal component $\hat{v}_0$ while the bottom row shows the spanwise component $\hat{w}_0$. The left, middle and right columns show the disturbances in the streamwise intervals $0 \leqslant x \leqslant 2$, $0 \leqslant x \leqslant 6$ and $0 \leqslant x \leqslant 10$, respectively. This figure reveals that there are significant differences between the optimal disturbance in the SSBL and the optimal disturbance in the ASBL. For the shortest streamwise interval, the shapes of the disturbance profiles differ, especially for the $\hat{w}$ component which is larger close to the wall in the SSBL than in the ASBL. For the longer intervals, the disturbances assume more or less the same shape, but the profile maxima are still located slightly higher

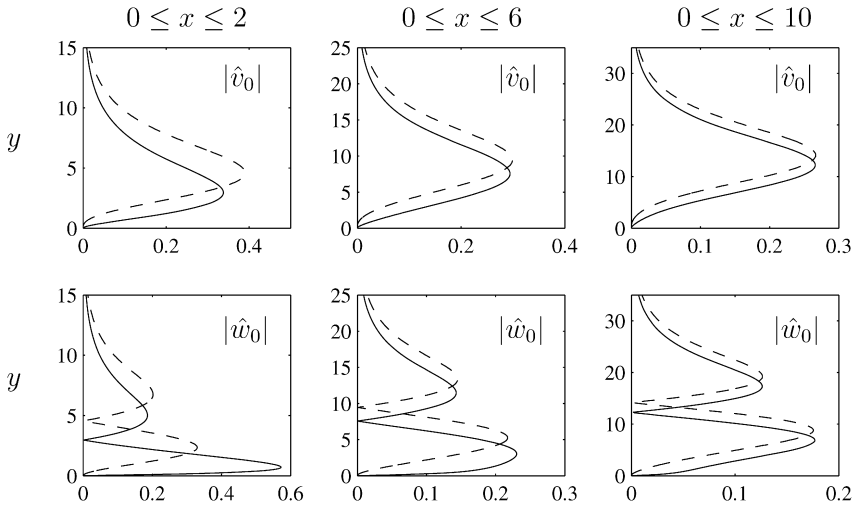

Fig. 10. The optimal disturbance in the SSBL (solid line) and the ASBL (dashed line) at $Re = 347$. The upper and bottom row shows respectively the wall-normal component $\hat{v}_0$ and the spanwise component $\hat{w}_0$.

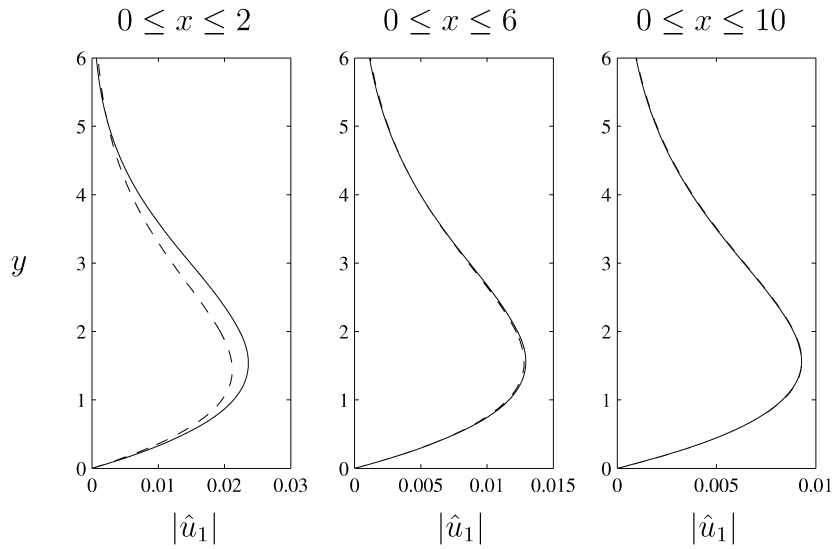

Fig. 11. The downstream response $\hat{u}_1$ of the optimal disturbance in the SSBL (solid line) and the ASBL (dashed line) at $Re = 347$.

in the ASBL than in the SSBL. This is due to the fact that the suction acts on the disturbance over a longer distance in the ASBL where the suction is applied over the whole interval. When the $\hat{v}$ and $\hat{w}$ components in the longest interval are plotted at $x = 1$ (not shown here), the disturbances in the ASBL and the SSBL almost collapse.

The optimal disturbance evolves downstream to the final position of the interval, shown in Fig. 11. The differences are now much smaller and only clearly visible for the shortest interval. There is no significant difference in the wall-normal distribution or shape of the disturbances, we conclude that for long intervals the downstream response of the optimal disturbance in the SSBL and the ASBL have the same shape and wall-normal distribution.

3.3. Comparison with experimental results

As previously mentioned, Fransson and Alfredsson [22] made an experimental study on the development and growth of disturbances induced into the SSBL by free-stream turbulence. The suction Reynolds numbers was $Re = 347$ and the suction started 360 mm downstream of the leading edge. Fransson and Alfredsson [22] found that the

spanwise wavenumber of the streaks depends on the level of the free-stream turbulence. Three grids were used to achieve different levels of turbulence; 1.4%, 2.2% and 4.0%. For these turbulence levels the measured spanwise wavenumbers were $\beta = 0.33$, $\beta = 0.41$ and $\beta = 0.47$, respectively. Fransson and Alfredsson [22] furthermore report that the spanwise scale of the streaks is maintained when suction is applied compared with the no-suction case. According to Fransson and Alfredsson [22], the initial spanwise scale is probably set by the receptivity process in the BBL at the leading edge of the SSBL. The optimal wavenumber in the ASBL is $\beta = 0.53$ [24] with temporal analysis and $\beta = 0.52$ with the spatial analysis presented herein. Fransson and Corbett [24] argue that the experimentally measured spanwise wavenumber approaches the optimal wavenumber as the free-stream turbulence level is increased. Their reasoning is that a high level of free-stream turbulence will provide enough energy over the whole range of scales to allow the boundary layer to amplify the disturbance with a wavenumber close to that of the optimal disturbance. There is however a discrepancy between the optimal and the measured wavenumber, even for the highest turbulence level. Fransson and Corbett [24] found good agreement between the downstream response to the optimal disturbance and experimentally measured disturbance profiles [22]. Equally good agreement was obtained with the present spatial analysis of the SSBL (not shown in figure).

In the present study the suction Reynolds number was set to $Re = 347$ and the suction was started at $x_s = 1$, emulating the base flow of the experiment by Fransson and Alfredsson [22]. In Section 3.1.2 it was shown that in this base flow the optimal growth decays when the endpoint of the interval is moved downstream of the point where the suction starts. The growth in the downstream region can therefore never surpass that obtained over the BBL in the upstream region where no suction is applied. The following hypothesis could therefore provide an explanation to why Fransson and Alfredsson [22] found that the spanwise scale of the streaks in the SSBL is close to the scale in the BBL. The free-stream turbulence contains a broad spectrum of spanwise scales, disturbances of scales close to the optimal scale in the BBL will experience the greatest growth and thus become dominating in the upstream region where no suction is applied. Other scales could however be present at the downstream position where the suction starts. It is possible that disturbances of different scales are continuously induced into the boundary layer downstream of the leading edge region, due to the forcing from the free-stream turbulence. Disturbances of scales close to the optimal in the ASBL should experience the greatest growth in the downstream region where suction is applied. There is however no possibility for these disturbances to grow and become dominating, since even disturbances of the optimal scale decay in the downstream region (Section 3.1.2). The streaks which dominated in the upstream region will therefore continue to dominate in the downstream region. This could explain why the experimentally observed streaks in the SSBL are of almost the same spanwise scale as those dominating in the BBL. The fact that the optimal growth decays in the downstream region is due to the relatively high suction rate used in the present study. Calculations with the present implementation have however shown that the maximum energy growth can be located downstream of the point where the suction starts, if the suction rate is sufficiently low. These results are not included in the present study since our primary interest lies in emulating the base flow of the experiments by Fransson and Alfredsson [22].

Yoshioka et al. [23] extended the study of Fransson and Alfredsson [22] to different turbulence levels, suction and free-stream velocities. For conditions close to those of the experiment by Fransson and Alfredsson [22], Yoshioka et al. [23] found that the disturbances are passively convected downstream without changing the spanwise scale. By simultaneously changing the suction and free-stream velocity, the suction Reynolds number was kept constant while the displacement thickness in the ASBL region was increased, thereby decreasing the difference in displacement thickness between the BBL upstream and the ASBL downstream. For these conditions, Yoshioka et al. [23] argue that the scale of the streaks approach the temporal optimal scale in the ASBL. In the current study it has been shown (Table 2) that the spanwise scale of the optimal disturbance in the ASBL depends on the streamwise interval length. Although the optimal scale in the optimal interval ($0 \leqslant x \leqslant 0.89$) is nearly identical to that found with temporal analysis [24], it is significantly wider in longer intervals.

To summarize, the experimental findings show that the spanwise scale of the streaks in the SSBL is close to the scale of the streaks in the BBL where no suction is applied. A possible explanation is provided in the current study, which shows that the relatively high suction rate makes it impossible for disturbances of the optimal scale in the ASBL to grow in the downstream region affected by suction. This region will therefore be dominated by streaks of scales close to the optimal scale in the BBL, since these disturbances have already grown to large amplitudes in the upstream region unaffected by suction. There are however important differences between the calculation of optimal disturbances presented herein and the experimental conditions. In the calculation of the optimal disturbance we assume that the disturbance enter the boundary layer at the initial point of the streamwise interval and then evolves

downstream without any influence from the outside disturbance environment. In the experiment the boundary layer is subjected to continuous forcing from the free-stream turbulence over the entire streamwise interval. It is also possible that nonlinear effects that are not accounted for in the calculation of the optimal disturbances occur in the experiment.

4. Conclusions

The energy growth of optimal disturbances was studied by means of linearized equations for the semi suction boundary layer (SSBL) and the asymptotic suction boundary layer (ASBL). The suction Reynolds number was set to 347.

Firstly, the algebraic growth in the SSBL was studied. It was found that the optimal disturbance consists of streamwise aligned vortex pairs that give rise to streamwise streaks. This disturbance gives rise to the highest possible growth when the streamwise interval ends at the point where the suction starts. The base flow of this optimal interval is the BBL, the optimal spanwise wavenumber in the SSBL is therefore the same as that in the BBL, $\beta = 0.45$ [15,16]. When the interval is prolonged beyond the starting point of the suction, the optimal spanwise wavenumber decreases, the optimal angular frequency is however zero irrespective of the interval length. Furthermore, it was found that the vortices, i.e. the optimal disturbance, grow as the interval is prolonged and that the cores of the vortices move upward in the wall-normal direction. This effect is due to the suction which draws the disturbance down towards the wall. The vortex cores must therefore be located higher initially in a long interval where the suction will act on the disturbance over a longer distance.

Secondly, the optimal disturbance in the ASBL was studied and a comparison with the SSBL was made. The optimal disturbance in the ASBL closely resembles that in the SSBL. The cores of the vortices, i.e. the optimal disturbance, are however located higher in the ASBL due to the fact that the suction acts on the disturbance over the whole streamwise interval. This difference vanishes as the disturbance evolves in the streamwise direction, the downstream response is therefore the same over long intervals. Furthermore, it was found that for short intervals the SSBL gives a significantly higher growth due to the contribution from the BBL. The optimal spanwise wavenumber was also lower for the SSBL than for the ASBL for these intervals. As the streamwise interval was prolonged the optimal growth and spanwise wavenumber in the SSBL approached those in the ASBL.

Finally, a comparison was made with experimental results from Fransson and Alfredsson [22] and Yoshioka et al. [23]. This comparison showed that both the experimental findings and the results presented herein support the theory that the spanwise scale of the disturbances is set in the BBL at the leading edge of the SSBL.

Acknowledgements

The authors thank Doctor J.H.M. Fransson who provided many insightful comments, from which this work has greatly benefited. We are indebted to Doctor P. Corbett, Professor A. Bottaro and Doctor J.H.M. Fransson who generously shared their code for temporal analysis of optimal disturbances.

References

[1] P.S. Klebanoff, Effect of freestream turbulence on the laminar boundary layer, Bull. Am. Phys. Soc. 10 (1971) 1323.
[2] K.J.A. Westin, A.V. Boiko, B.G.B. Klingmann, V.V. Kozlov, P.H. Alfredsson, Experiments in a boundary layer subjected to free stream turbulence. Part 1. Boundary layer structure and receptivity, J. Fluid Mech. 281 (1994) 193–218.
[3] M. Matsubara, P.H. Alfredsson, Disturbance growth in boundary layers subjected to free-stream turbulence, J. Fluid Mech. 430 (2001) 149–168.
[4] J.H.M. Fransson, M. Matsubara, P.H. Alfredsson, Transition induced by free-stream turbulence, J. Fluid Mech. 527 (2005) 1–25.
[5] P. Andersson, L. Brandt, A. Bottaro, D.S. Henningson, On the breakdown of boundary layer streaks, J. Fluid Mech. 428 (2001) 29–60.
[6] L. Brandt, D.S. Henningson, Transition of streamwise streaks in zero-pressure-gradient boundary layers, J. Fluid Mech. 472 (2002) 229–261.
[7] J. Hœpffner, L. Brandt, D.S. Henningson, Transient growth on boundary layer streaks, J. Fluid Mech. 537 (2005) 91–100.
[8] M.T. Landahl, Wave breakdown and turbulence, SIAM J. Appl. Math. 28 (4) (1975) 735–756.
[9] M.T. Landahl, A note on an algebraic instability of inviscid parallel shear flows, J. Fluid Mech. 98 (2) (1980) 243–251.
[10] T. Ellingsen, E. Palm, Stability of linear flow, Phys. Fluids 18 (4) (1975) 487–488.
[11] K.M. Butler, V.F. Farrell, Three-dimensional optimal perturbations in viscous shear flow, Phys. Fluids A 4 (8) (1992) 1637–1650.
[12] S.C. Reddy, D.S. Henningson, Energy growth in viscous channel flows, J. Fluid Mech. 252 (1993) 209–238.
[13] P. Corbett, A. Bottaro, Optimal perturbations for boundary layers subject to stream-wise pressure gradient, Phys. Fluids 12 (1) (2000) 120–130.
[14] P. Corbett, A. Bottaro, Optimal linear growth in swept boundary layers, J. Fluid Mech. 435 (2001) 1–23.

[15] P. Andersson, M. Berggren, D.S. Henningson, Optimal disturbances and bypass transition in boundary layers, Phys. Fluids 11 (1) (1999) 134–150.
[16] P. Luchini, Reynolds-number-independent instability of the boundary layer over a flat surface: optimal perturbations, J. Fluid Mech. 404 (2000) 289–309.
[17] O. Levin, D.S. Henningson, Exponential vs algebraic growth and transition prediction in boundary layer flow, Flow, Turbulence and Combustion 70 (2003) 183–210.
[18] P. Balakumar, P. Hall, Optimum suction distribution for transition control, Theoret. Comput. Fluid Dynamics 13 (1999) 1–19.
[19] J.O. Pralits, A. Hanifi, D.S. Henningson, Adjoint-based optimization of steady suction for disturbance control in incompressible flows, J. Fluid Mech. 467 (2002) 129–161.
[20] S. Zuccher, P. Luchini, A. Bottaro, Algebraic growth in a Blasius boundary layer: optimal and robust control by mean suction in the nonlinear regime, J. Fluid Mech. 513 (2004) 135–160.
[21] H. Schlichting, Boundary-Layer Theory, seventh ed., McGraw-Hill, 1979.
[22] J.H.M. Fransson, P.H. Alfredsson, On the disturbance growth in an asymptotic suction boundary layer, J. Fluid Mech. 482 (2003) 51–90.
[23] S. Yoshioka, J.H.M. Fransson, P.H. Alfredsson, Free stream turbulence induced disturbances in boundary layers with wall suction, Phys. Fluids 16 (11) (2004) 3530–3539.
[24] J.H.M. Fransson, P. Corbett, Optimal linear growth in the asymptotic suction boundary layer, Eur. J. Mech. B Fluids 22 (2003) 259–270.
[25] A.A. Griffith, F.W. Meredith, The possible improvement in aircraft performance due to boundary layer suction, Tech. Rep. 2315, Rep. Aero. Res. Coun., 1936.
[26] P.J. Schmid, D.S. Henningson, Stability and Transition in Shear Flows, Springer, 2001.
[27] P. Corbett, A. Bottaro, Optimal control of nonmodal disturbances in boundary layers, Theoret. Comput. Fluid Dynamics 15 (2001) 65–81.
[28] S. Berlin, D.S. Henningson, A nonlinear mechanism for receptivity of free-stream disturbances, Phys. Fluids 11 (12) (1999) 3749–3760.
[29] D. Biau, A. Bottaro, Transient growth and minimal defects: Two possible initial paths of transition to turbulence in plane shear flows, Phys. Fluids 16 (10) (2004) 3515–3529.